Sharma, O. K., & Kerr, S. J. (1979) *Biochem. Biophys. Res. Commun. 87*, 1039–1043.
Sharma, O. K., Borek, E., & Martinez-Hernandez, A. (1976) *Nature (London) 259*, 588–591.
Shaw, G., & Kamen, R. (1986) *Cell (Cambridge, Mass.) 46*, 659–667.
Shepherd, J. H., Mulvihill, E. R., Thomas, P. S., & Palmiter, R. D. (1980) *J. Cell. Biol. 87*, 142–151.
Silverman, R. H. (1985) *Anal. Biochem. 144*, 450–460.
Silverman, R. H., Skehel, J. J., James, T. C., Wreschner, D. H., & Kerr, I. M. (1983) *J. Virol. 46*, 1051–1055.
Sokawa, J., Shimizu, N., & Sokawa, Y. (1984) *J. Biochem. (Tokyo) 96*, 215–222.
Stark, G. R., Dower, W. J., Schimke, R. T., Brown, R. E., & Kerr, I. M. (1979) *Nature (London) 278*, 471–473.
Swaneck, G. E., Nordstrom, J. L., Kreuzaler, F., Tsai, M. J., & O'Malley, B. W. (1979) *Proc. Natl. Acad. Sci. U.S.A. 76*, 1049–1053.
Vannice, J. L., Taylor, J. M., & Ringold, G. M. (1984) *Proc. Natl. Acad. Sci. U.S.A. 81*, 4241–4245.
Watling, D., Serafinowska, H. T., Reese, C. B., & Kerr, I. M. (1985) *EMBO J. 4*, 431–436.
Williams, B. R. G., Golgher, R. R., Brown, R. E., Gilbert, C. S., & Kerr, I. M. (1979) *Nature (London) 282*, 582–586.
Wiskocil, R., Bensky, P., Dower, W., Goldberger, R. F., Gordon, J. I., & Deeley, R. G. (1980) *Proc. Natl. Acad. Sci. U.S.A. 77*, 4474–4478.
Yang, K., Samanta, H., Dougherty, J., Jayaram, B., Broeze, R., & Lengyel, P. (1981) *J. Biol. Chem. 256*, 9324–9328.

A Monomer–Dimer Model Explains the Results of Radiation Inactivation: Binding Characteristics of Insulin Receptor Purified from Human Placenta†

Yoko Fujita-Yamaguchi* and Joan T. Harmon‡

Department of Molecular Genetics, Beckman Research Institute of the City of Hope, 1450 East Duarte Road, Duarte, California 91010, and Molecular Biology Laboratories, Jerome H. Holland Laboratory, American Red Cross, 15601 Crabbs Branch Way, Rockville, Maryland 20855

Received October 1, 1987; Revised Manuscript Received January 5, 1988

ABSTRACT: The technique of radiation inactivation has been used on highly purified human placental insulin receptor in order to determine the functional molecular size responsible for the insulin binding and to evaluate the "affinity regulator" hypothesis, which has been proposed to explain the increase in specific insulin binding to rat liver membranes observed at low radiation doses [Harmon, J. T., Hedo, J. A., & Kahn, C. R. (1983) *J. Biol. Chem. 258*, 6875–6881]. Three different types of inactivation curves were observed: (1) biphasic with an enhanced binding activity after exposure to low radiation doses, (2) nonlinear with no change in binding activity after exposure to low radiation doses, and (3) linear with a loss in the binding activity with increasing radiation exposures. A monomer–dimer model was the simplest model that best described the three types of radiation inactivation curves observed. The model predicts that an increase in insulin binding activity would result after exposure to low radiation doses when the initial dimer/monomer ratio is equal to or greater than 1 and a monomer is more active than a dimer. The monomer size of the binding activity was estimated to be 227 000 daltons by this model. This value most likely reflects the size of the monomeric $\alpha\beta$ form. To substantiate this model, the purified receptor was fractionated by Sepharose CL-6B chromatography. The insulin binding profile of this column indicated two peaks. Further studies revealed the following: (i) peak I ($\alpha_2\beta_2$-rich) and peak II ($\alpha\beta$-rich) receptors showed curvilinear Scatchard plots and straight Scatchard plots, respectively, and (ii) specific activity of the peak I receptors was estimated to be 26% of that of the peak II receptors under our standard conditions [50 mM tris(hydroxymethyl)aminomethane hydrochloride, pH 7.4]. These studies suggest that the affinity regulator does not exist as a separate structural protein but is due to the dimeric form of the receptor. The dimeric form ($\alpha_2\beta_2$) possesses a much lower specific activity for insulin binding than does the monomeric $\alpha\beta$ form (under the standard conditions), but the dimeric structure is necessary to observe the negative cooperative binding isotherm.

The insulin receptor is a membrane glycoprotein that is responsible for transferring the signal from the exterior to the interior of target cells and leading to insulin-dependent biological actions (Kahn et al., 1981). The structure of the receptor has been studied by a variety of techniques. These studies have indicated that the basic insulin receptor unit is composed of two α subunits and two β subunits in a β–α–α–β form (Jacobs et al., 1979; Maturo & Hollenberg, 1978; Yip et al., 1980; Pilch & Czech, 1980; Czech et al., 1981; Baron & Sonksen, 1983).

The technique of radiation inactivation can be used to ascertain the size of the functional unit, for example, the insulin binding site, corresponding to a given biological activity, insulin binding. When high-energy radiation causes ionization in a

† This work was supported by Research Grants DK29770 and DK34437 (to Y.F.-Y.) and HL37519 (to J.T.H.) from the National Institutes of Health.
* Correspondence should be addressed to this author at the Beckman Research Institute of the City of Hope.
‡ American Red Cross.

0006-2960/88/0427-3252$01.50/0

molecule, there is a radiation-dependent loss of biological activity that is proportional to the mass of the functional unit (Harmon et al., 1985). By use of this technique, the structure of the insulin receptor in situ in rat liver membranes has been studied (Harmon et al., 1980, 1981). Since the radiation inactivation curve showed an ~2-fold increase in specific insulin binding over the first 12-Mrad[1] dose, it was proposed that the receptor is composed of at least two functional components, an affinity regulator (M_r 300 000) and a binding component (M_r 100 000), and that the affinity regulator interacts with the binding component, to cause a decrease in receptor affinity in situ. Further studies suggested that the affinity regulator is a membrane protein, associated with the binding component. After partial purification, the affinity of the binding component is elevated, suggesting either the removal or the inactivation of the affinity regulator (Harmon et al., 1983). The same technique was applied to solubilized human lymphoblastoid cell IM-9 by Pollet et al. (1982), who did not observe the changes associated with an affinity regulator but instead observed a monoexponential decrease in the number of active receptors with increasing radiation dose, indicating a single-size binding unit of M_r 170 000 for the insulin binding component. Although the discrepancy between the results reported by the two groups has been suggested to be due to tissue specificity, this has not been clearly resolved.

We have previously purified the insulin receptor from human placenta to apparent homogeneity (Fujita-Yamaguchi et al., 1983) and determined its subunit structure (Fujita-Yamaguchi, 1984). This receptor preparation not only has high insulin binding activity but also exhibits tyrosine protein kinase activity (Kasuga et al., 1983; Fujita-Yamaguchi & Kathuria, 1985). Affinity labeling experiments and cloning studies of the insulin receptor from different laboratories (Massague et al., 1980; Roth & Cassell, 1983; Ullrich et al., 1985; Ebina et al., 1985) have suggested that the α subunits contain the insulin binding site whereas the β subunits possess the tyrosine kinase activity. We have now used the technique of radiation inactivation on our purified insulin receptor in order to examine potential functional interactions between these subunits and thus to define the nature of the affinity regulation. Our new results suggest that the purified insulin receptor preparations contain monomeric $\alpha\beta$ forms and dimeric $\alpha_2\beta_2$ forms which exist in equilibrium and that the insulin binding activity of the monomer is higher than that of the dimer. We then tried to validate this interpretation of radiation inactivation data by a different biochemical approach, based on the recent results of Koch et al. (1986), who show the existence of two insulin receptor species with different binding properties in rat liver microsomal Triton extracts. When the rat liver receptors were fractionated by Sepharose CL-6B chromatography, the insulin binding profiles appeared different depending on assay conditions used; buffers of high molarity and basic pH yielded both peak I and peak II whereas buffers of low molarity and neutral pH yielded peak II only. Cross-linking of the receptor species with ^{125}I-insulin followed by SDS–PAGE analysis indicated that peaks I and II correspond to $\alpha_2\beta_2$ and $\alpha\beta$ receptors, respectively. Since our binding assay conditions are similar to the "buffers of low molarity and neutral pH" described by Koch et al., it is plausible to assume that the peak II (monomeric) receptor is more active than the peak I (dimeric) receptor. Therefore, we have extended our findings from radiation inactivation experiments by examining affinity-purified insulin receptors using Sepharose CL-6B chromatography. These studies revealed unique characteristics of the insulin receptor binding activity which is determined by the dimer ($\alpha_2\beta_2$)–monomer ($\alpha\beta$) ratio since the monomeric form exhibits higher insulin binding activity than the dimeric form under our standard conditions. Such studies described in this paper can be generally applied to radiation inactivation analyses of protein mixtures that interact with each other and contribute to a given biological activity.

[1] Abbreviations: SDS–PAGE, sodium dodecyl sulfate–polyacrylamide gel electrophoresis; BSA, bovine serum albumin; Mrads, megarads; Tris-HCl, tris(hydroxymethyl)aminomethane hydrochloride; PMSF, phenylmethanesulfonyl fluoride; WGA, wheat germ agglutinin; PEG, poly(ethylene glycol).

Materials and Methods

Materials. Crystalline porcine insulin was supplied by Eli Lilly; Iodo-Beads were purchased from Pierce Chemical Co.; Sepharose CL-6B was purchased from Pharmacia; thyroglobulin, catalase, γ-globulin, and calf intestine alkaline phosphatase were obtained from Sigma; ^{125}I-labeled insulin and Na^{125}I were purchased from New England Nuclear. All other chemicals used were reagent grade.

Preparation of Triton X-100 Membrane Extracts and Purification of the Insulin Receptor. Triton X-100 extracts of human placental membranes and purified insulin receptor were prepared as previously described (Fujita-Yamaguchi et al., 1983). Briefly, placental membranes (25 mg/mL) were solubilized by stirring in 50 mM Tris-HCl buffer, pH 7.4, containing 2% Triton X-100 and 0.1 mM PMSF for 45 min at room temperature. The Triton X-100 membrane extracts were obtained as a clear supernatant by centrifugation at 100000g for 90 min at 4 °C. The insulin receptor was purified 2400-fold with a yield of 40% from the Triton X-100 membrane extracts by sequential affinity chromatography on wheat germ agglutinin–Sepharose and insulin–Sepharose columns.

Insulin Binding Assay (Standard Conditions). Insulin binding activity was measured by incubating the receptor preparation at 4 °C for 16 h with ^{125}I-labeled porcine insulin (20 000 cpm, 0.2 ng) in a final volume of 0.4 mL of 50 mM Tris-HCl buffer, pH 7.4, containing 0.1% Triton X-100 and 0.1% bovine serum albumin in the absence and presence of excess unlabeled porcine insulin (20 μg/mL). For the competition binding assay, various amounts of unlabeled insulin were added to the reaction mixtures to give a final concentration of 0.1–200 ng/mL. The receptor–^{125}I-insulin complex was separated from free ^{125}I-insulin by adding 0.1 mL of 0.4% bovine γ-globulin and 0.5 mL of 20% poly(ethylene glycol) 6000, followed by centrifuging at 1500g for 20 min at 4 °C. The supernatants were aspirated, and the pellets were counted with a γ counter.

The data from competition experiments were subjected to computer analysis by weighted nonlinear least-squares curve fitting, with total ligand concentration as the independent variable, using the program LIGAND (Munson & Rodbard, 1984). Different models were considered: a one-site model without cooperative interactions, a one-site model with cooperative interactions, a two-site model, and a two-site model in which one of the sites is involved in cooperative interactions. Objective statistical criteria (F test, extra sum of squares principle) were used to evaluate goodness of fit and for discriminating beween different models. Nonspecific binding was treated as a parameter subject to error and was fitted simultaneously with other parameters. Results were displayed graphically by the method of Scatchard (1949).

Iodination of the Insulin Receptor and Evaluation of the PEG Precipitation Method. The purifed insulin receptor was iodinated by the chloramine T method as described previously (Fujita-Yamaguchi et al., 1986), or alternatively by using

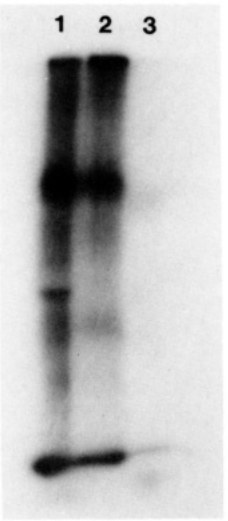

FIGURE 1: SDS–PAGE analysis of ^{125}I-labeled insulin receptor before and after PEG precipitation. Highly purified insulin receptor (20 ng) that had been ^{125}I-labeled was precipitated by the PEG procedure as described under Materials and Methods. The precipitate and the supernatant were analyzed by SDS–PAGE (7.5% gel) under reducing conditions (lanes 2 and 3, respectively). The same amount of ^{125}I-labeled receptor used for PEG precipitation is shown in lane 1.

Iodo-Beads according to the method of Markwell (1982).

Since it has been suggested by others that only a fraction of the insulin receptors can be precipitated by PEG precipitation (Finn et al., 1984), ^{125}I-labeled purified insulin receptor (20 ng) was subjected to PEG precipitation under our conditions as described above. The resulting precipitate and supernatant were analyzed by SDS–polyacrylamide gel electrophoresis (Figure 1, lanes 2 and 3) together with the same amount of ^{125}I-labeled insulin receptor without PEG treatment (Figure 1, lane 1). The results show that, in contrast to the previous report, the receptor is quantitatively precipated by PEG.

Gel Filtration Chromatography on Sepharose CL-6B. The purified insulin receptor (~5–10 μg) was applied to a Sepharose CL-6B column (1.5 × 50 cm) and eluted with 10 mM Tris-HCl buffer, pH 7.4, containing 0.1% Triton X-100. Fractions of 1 mL each were collected, and 100-μL aliquots were assayed for specific insulin binding under two conditions: (i) 50 mM Tris-HCl buffer, pH 7.4, containing 0.1% Triton X-100 and 0.1% BSA (our standard conditions) or (ii) 60 mM phosphate buffer, pH 8.0, containing 0.2 M Na_2SO_4, 0.1% Triton X-100, and 0.1% BSA (Koch et al., 1986).

The receptor (~5 ng) which had been iodinated was applied to the column. The aliquots (50 μL) of fractions were analyzed by SDS–polyacrylamide (7.5%) gel electrophoresis performed under nonreducing conditions (Laemmli, 1970). The gels were prepared for autoradiography. The radioactive peaks were quantitated by densitometric scanning by using a Beckman DU-50 spectrophotometer.

For molecular size determinations, thyroglobulin, catalase, γ-globulin, and calf intestine alkaline phosphatase were used and assayed as described (LeBon et al., 1986).

Irradiation Procedure. The samples in sealed ampules were irradiated with 13-MeV electrons from a linear accelerator (Armed Forces Radiobiology Research Institute, Bethesda, MD) as previously described (Harmon et al., 1980). The temperature of the sample during irradiation was maintained at −130 ± 5 °C.

Theory and Calculations. The results of radiation inactivation studies were analyzed by classical target theory as previously described (Harmon et al., 1980, 1985). Briefly, the logarithm of the fraction of remaining specific insulin binding (using the bound/free ratio) was plotted versus exposure dose. The following models were considered:

(*A*) *Single-Site Model.* In the simplest situation when only one component is responsible for the total activity, the inactivation curve is assumed to be a single exponential. In this case, the molecular weight of the binding component can be calculated as previously described by using the formula:

$$M_r = (6.4 \times 10^5) S_t K$$

where S_t is a temperature correction of 2.8 (Harmon et al., 1983; Schlegel et al., 1979) and K is the slope of the radiation inactivation curve with the dose measured in megarads (Mrad). The slope of the radiation inactivation curve is obtained from the best-fit line generated by the use of a computer program (RS/1, BBW Research Systems, Cambridge, MA) for weighted nonlinear regression.

(*B*) *Multisite Model.* When several components of different functional sizes contribute to the total activity, the radiation inactivation curve is multiexponential. The data can be fit to the equation:

$$A/A_0 = F_1 e^{-K_1 r} + F_2 e^{-K_2 r} + \ldots + F_n e^{-K_n r}$$

where A is the activity measured at given radiation dose, A_0 is the activity of the unirradiated control, F_1, F_2, ..., F_n are the fractions of activity contributed by each functional unit(n) ($F_1 + F_2 + \ldots + F_n = 1.0$), K_1, K_2, ..., K_n are the slopes of the inactivation curve for each n unit, and r is the radiation dose. For an apparent single exponential inactivation curve, n equals 1.

(*C*) *Monomer–Dimer Model.* The following equation derived for the analysis of radiation inactivation data on calmodulin-independent phosphodiesterase activity (Kincaid et al., 1981) was used to analyze our data:

$$A/A_0 = e^{-K_m r}[1 + (D_0/M_0)(1 - e^{-2K_m r})] \qquad (1)$$

where A_0 is an initial activity and A is the activity at dose r (in Mrad). The equation involves the following assumptions: (1) Before irradiation, the receptor preparation contains a certain ratio of monomers (M_0) and dimers (D_0). (2) Monomers are fully active and dimers are totally inactive. (3) Upon radiation destruction of a dimer, an active monomer is generated. (This assumption does not take into account the possibility that radiation may, in some cases, damage both subunits.) (4) The functional size of a dimer is twice that of a monomer.

A variation of this model has also been examined in which the dimer does have activity. This model is described as

$$A = (1 - Z)[e^{-K_m r} + (D_0/M_0)e^{-K_m r}(1 - e^{-2K_m r})] + Ze^{-2K_m r} \qquad (2)$$

where Z is the fraction of total activity associated with the dimer in the control, unirradiated sample.

RESULTS

Effect of Radiation on Insulin Binding Activity of Triton X-100 Extracts of Placental Membranes. When Triton X-100 extracts of placental membranes were irradiated, an increase (~30–100%) in specific insulin binding was observed. The results from one experiment are shown in Figure 2. This increase in binding activity is shown, from Scatchard analysis, to be caused by an enhancement in the affinity of the binding component (data not shown). These results are consistent with previous observations by Harmon et al. (1980, 1981) with rat liver membranes but do not agree with the results reported by Pollet et al. (1982) using lymphoblastoid cells. However, it should be noted that the fraction of remaining active re-

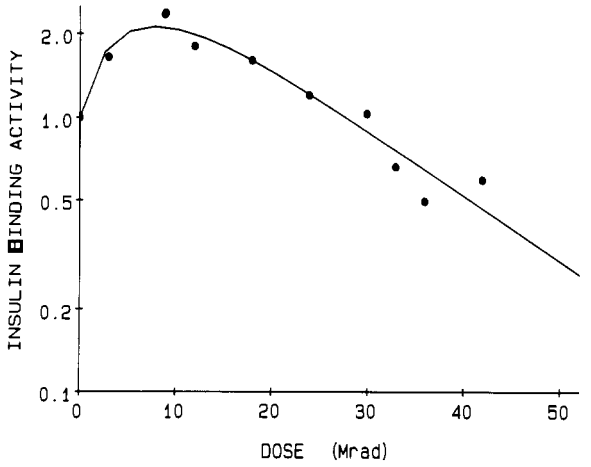

FIGURE 2: Inactivation of ^{125}I-insulin binding to Triton X-100 solubilized human placental membrane. The solubilized membrane fraction (8.2 mg/mL) was irradiated at −135 °C with high-energy electrons, and then 3-μL aliquots were assayed for ^{125}I-insulin binding at a concentration of 0.1 nM insulin. The data shown are from a single experiment but are representative of three separate irradiations for the solubilized membrane. Insulin binding [$(B/F)/(B/F)_0$, where (B/F) is the remaining insulin binding at a given dose of radiation divided by $(B/F)_0$ for the nonirradiated control] is plotted versus exposure dose. Data fit to a monomer–dimer model where dimers have no activity.

Table I: Target Size Analysis of Insulin Binding to the Purified Insulin Receptor[a]

preparation	type of radiation inactivation curve[b]	M_r[c]	D_0/M_0 ratio[c]
1	B	274000	0.69
2	A	161000	1.80
3[d]	C	233000	0.20
4	C	222000	0.34
5	C	217000	0.15
6	A	255000	2.10
mean		227000 ± 39000	

[a] The samples frozen during irradiation were thawed and assayed immediately. [b] The three types of radiation inactivation curves are shown in Figure 3. [c] The functional size for insulin binding site (M_r) and a dimer/monomer (D_0/M_0) ratio were estimated by a monomer–dimer model (eq 1) as described under Materials and Methods. [d] For this experiment, the receptor was purified from freshly prepared placental membranes. The receptor for the rest of the experiments was purified from frozen placental membranes.

ceptors after irradiation determined from the Scatchard analysis (R/R_0) gave a linear radiation inactivation curve corresponding to a size of 110000 daltons (data not shown) since R/R_0 is not influenced by the receptor affinity whereas insulin binding measured at a tracer concentration of ^{125}I-insulin reflects both receptor number and affinity. The results of radiation inactivation experiments on Triton X-100 extracts of human placental receptors are subjected to analysis by the monomer–dimer model (assuming inactive dimer, see below), which results in the average functional size for the insulin binding site being 102000 ± 14000 daltons (n = 3).

Effect of Radiation on Insulin Binding Activity of the Purified Insulin Receptor. (A) Radiation Inactivation of the Purified Insulin Receptor. Following radiation inactivation, samples of the highly purified receptor were thawed and immediately assayed for insulin binding activity. Three different types of radiation inactivation curves were obtained: in two of the six preparations examined (Table I, preparations 2 and 6) a biphasic radiation inactivation curve (Figure 3A) was obtained, reflecting enhanced binding activity after exposure to low radiation doses (<6 Mrad) due to an increase in the

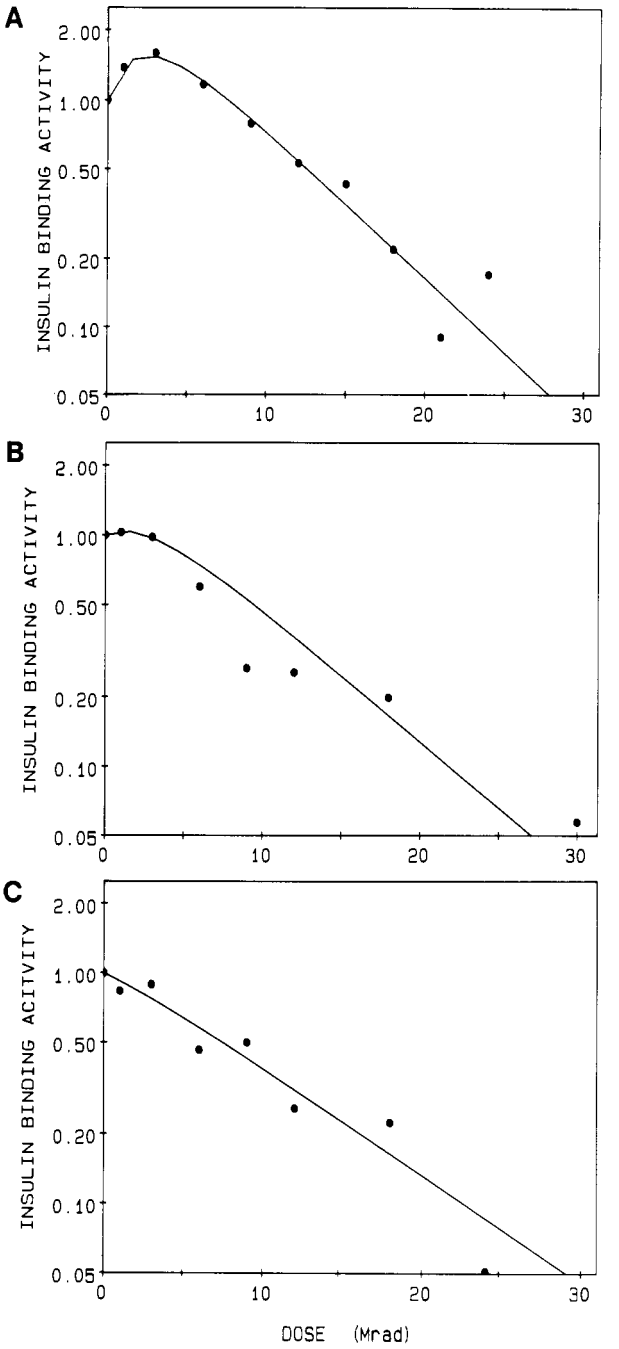

FIGURE 3: Summary of the results of target size analyses on insulin binding activity of purified insulin receptor. The fraction of remaining insulin binding $(B/F)/(B/F)_0$ is plotted versus exposure dose. Three types of inactivation curve were observed as summarized in Table I: A, biphasic type (preparation 6); B, nonlinear type (preparation 2); and C, linear type (preparation 4).

affinity of binding (Scatchard analysis data not shown); with one preparation (Table I, preparation 1) there was a nonlinear inactivation curve (Figure 3B) with virtually no loss in binding activity after low radiation exposure; and with three other preparations (Table I, preparations 3–5) there was an apparent linear radiation inactivation curve (Figure 3C).[2] Scatchard analysis of these latter receptor preparations indicated a decrease in the number of binding sites without an obvious change in the affinity of the remaining sites to bind insulin (data not shown).

[2] It should be noted that these inactivation curves are not completely linear since, as expected, there are some dimers in the preparations (D_0/M_0 ratio is not 0, see below).

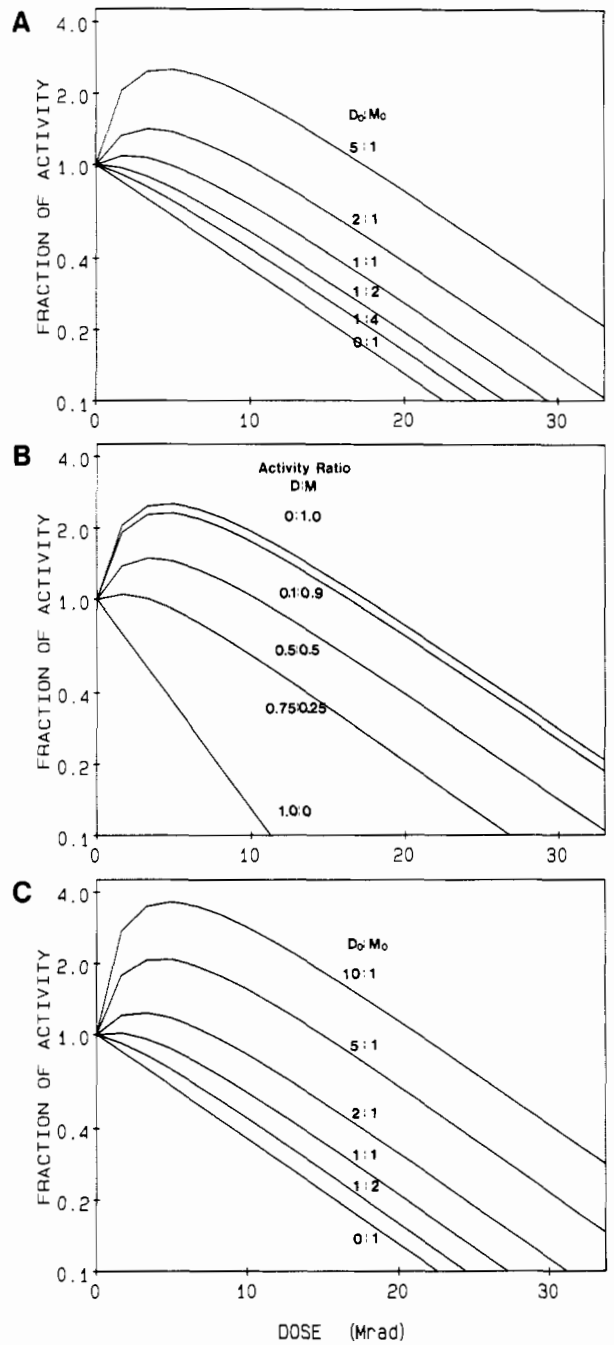

FIGURE 4: Effect of radiation on ^{125}I-insulin binding to the purified insulin receptor simulated by a computer analysis. (A) Dimer–monomer with dimer having no activity. Equation 1 described under Materials and Methods was used; D_0/M_0 is varied as indicated. (B) Dimer–monomer model with dimer having activity. Equation 2 described under Materials and Methods was used; D_0/M_0 = 5:1 is set constant. Z (initial activity of the dimer) is varied as shown by D/M activity ratio. (C) Dimer–monomer model with dimer having activity. Equation 2 described under Materials andMethods was used; Z (initial activity of the dimer) is held constant at 0.2. D_0/M_0 is varied as indicated.

Although these three different types of curves at first sight look like disparity in data, it turns out from the following data analysis that they represent minor variability within a unique simple model.

(*B*) *Data Analysis.* Several mathematical models were examined for their ability to generate the various radiation inactivation curves observed with the purified insulin receptor. These models included (1) a single functional unit model, (2) a multiple functional unit model, (3) a monomer–dimer model in which the dimer has no activity but the monomer does, and (4) a monomer–dimer model in which the dimer and monomer have activity. The single functional unit model was immediately discarded because enhanced activity after exposure to low radiation doses cannot occur with this model. The multiple functional unit model or the affinity regulator/binding component model was also discarded because the purified insulin receptor preparations contained, as judged by SDS–PAGE analysis (Fujita-Yamaguchi, 1984), no separate large molecular weight component that would coincide with the affinity regulatory component. Two variations of a monomer–dimer model were therefore considered: in one variation, the dimer has no activity, and in the second variation, the dimer has activity. Both of these variations can generate enhanced binding activity after exposure to low doses of radiation.

Table II: Comparison of Insulin Binding Activity of the Two Receptor Species Fractionated by Sepharose CL-6B Chromatography

	specific activity[a] for expt			
	1	2	3	mean
peak I	0.52	0.58	0.74	
peak II	2.29	2.09	2.60	
ratio of activities (peak I/peak II)	0.23	0.28	0.28	0.26 ± 0.02

[a] Specific insulin binding was measured in 50 mM Tris-HCl buffer, pH 7.4, containing 0.1% Triton X-100 and 0.1% BSA. Specific activity is expressed as % specific insulin binding/μg of protein.

Computer-simulated radiation inactivation curves for these two model variations are shown in Figure 4. The projection for the monomer–dimer model in which the dimer has no intrinsic activity (Figure 4A) indicates that a dimer to monomer ratio of 1 or greater results in enhanced binding after exposure to low radiation doses. The magnitude of this enhancement is proportional to the D_0/M_0 ratio. In the absence of dimer (D_0/M_0 = 0:1), the inactivation curve is linear with a slope determined by the functional size of the monomer. Thus, after exposure to higher doses of radiation, all the inactivation curves become parallel with a slope reflecting the monomer size irrespective of the D_0/M_0 ratio.

The second variation of monomer–dimer model in which the dimer has intrinsic activity requires an additional term (Z) to be added to the equation to allow for the fraction of total activity contributed by the dimer. If the dimer to monomer ratio is held constant (5:1) and the fraction of activity contributed by the dimer is varied, the inactivation curves shown in Figure 4B are obtained. As the proportion of activity contributed by the dimer increases, the enhancement of activity observed after exposure to low radiation doses decreases. The computer analyses indicate that a dimer/monomer activity ratio of 3 or less results in enhanced binding after expossure to low radiation dose. In the extreme, all the activity is attributable to the dimer (Z = 1.0). Now, the slope of the inactivation curve is twice as steep because it represents the functional size of the dimer instead of the monomer (the steeper the slope, the higher the molecular weight). In contrast, if the dimer to monomer ratio is held equal (1:1), an enhancement of activity after low radiation doses is hardly seen unless Z = 0 (see Figure 4A,C).

Alternatively, if the fraction of total activity contributed by the dimer is held constant at 0.2 and the ratio of dimer to monomer is varied, the projections shown in Figure 4C are obtained. This fraction of total activity was used in these calculations to correspond with the results obtained upon separation of dimers and monomers by size exclusion chromatography (Table II). As the dimer to monomer ratio decreases, the enhancement in activity observed after exposure to low radiation doses decreases. In other words, when the

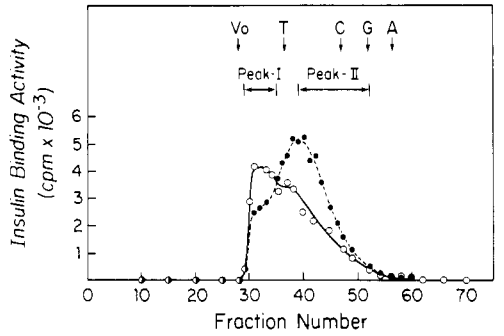

FIGURE 5: Gel filtration chromatography of purified insulin receptor on Sepharose CL-6B. The purified receptor (~5–10 μg) was applied to a Sepharose CL-6B column (1.5 × 50 cm) and eluted with 10 mM Tris-HCl buffer, pH 7.4, containing 0.1% Triton X-100. Fractions of 1 mL each were collected, and 100-μL aliquots were assayed for specific insulin binding under two conditions; (i) 50 mM Tris-HCl buffer, pH 7.4, containing 0.1% Triton X-100 and 0.1% BSA (●) or (ii) 60 mM phosphate buffer, pH 8.0, containing 0.2 M Na_2SO_4, 0.1% Triton X-100, and 0.1% BSA (○). Molecular size markers indicated are thyroglobulin (T), catalase (C), γ-globulin (G), and calf intestine alkaline phosphatase (A).

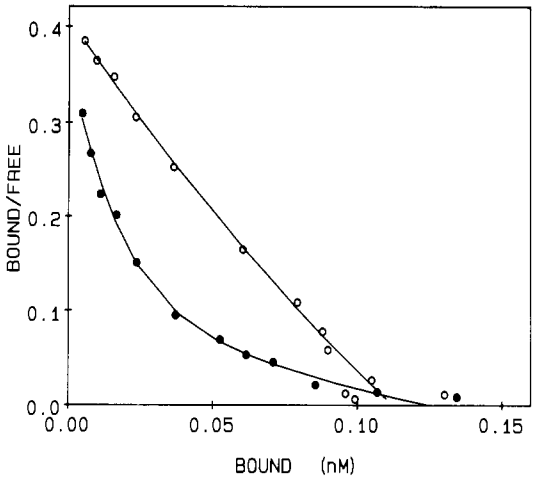

FIGURE 6: Scatchard analysis of peak I and II receptors. Peaks I and II were pooled as described in Figure 5. Competition insulin binding assays were performed with 100-μL aliquots under the standard conditions (50 mM Tris-HCl buffer, pH 7.4, containing 0.1% Triton X-100 and 0.1% BSA) as described under Materials and Methods. Peak I fraction (●) was best described by a two-site model in which one of the sites was involved in cooperative interactions. Peak II fraction (○) was best described by a one-site model.

concentration of dimer drops to zero, the radiation inactivation curve appears linear with a slope determined by the size of the monomer. Thus, the model variation in which the dimer has intrinsic activity has two parameters that are very dependent on each other: the ratio of dimer to monomer and the fraction of total activity contributed by the dimer. In the absence of experimental procedures to accurately determine either parameter alone, we have used the monomer–dimer model variation in which the dimer has no intrinsic activity to analyze the radiation inactivation curves presented here. However, it should be noted that whichever model variation was used, the functional sizes obtained were not significantly different.

(*C*) *The Functional Size for the Insulin Binding Site.* The functional size for insulin binding activity was estimated to be 227 000 ± 39 000 daltons by the monomer–dimer model (Table I), with the dimer being 454 000 daltons. The monomer size most likely reflects half the size of the intact $\alpha_2\beta_2$ receptor since the molecular weight of the half-receptor has been estimated as 195 000 by SDS–PAGE (Fujita-Yamaguchi, 1984).

Separation and Characterization of Monomers and Dimers. The radiation inactivation studies on the purified insulin receptor described above suggested that (i) the receptor preparations are composed of a mixture of monomers and dimers and (ii) a monomer has a higher specific insulin binding than a dimer. In order to compare the insulin binding activity of monomers and dimers, the affinity-purified receptor was applied to a Sepharose CL-6B column. Insulin binding was measured under the standard conditions (50 mM Tris-HCl buffer, pH 7.4, containing 0.1% Triton X-100) as well as at pH 8.0 with high salt conditions (60 mM phosphate buffer, pH 8.0, containing 0.1% Triton X-100 and 0.2 M Na_2SO_4), which were recently shown to give a higher insulin binding affinity of $\alpha_2\beta_2$ receptors (Koch et al., 1986). As shown in Figure 5, two insulin binding peaks that migrated at ~9.2 nm (peak I) and ~8.0 nm (peak II) were detected. They appear to correspond with $\alpha_2\beta_2$ and $\alpha\beta$ receptors, respectively, both of which were previously described to be present in solubilized liver membrane receptors (Koch et al., 1986). Indeed, when ^{125}I-labeled receptors were applied to the same column and the eluates were analyzed by SDS–PAGE under nonreducing conditions, we found that the dimers elute first as a peak followed by a peak of monomers although a complete separation of the two peaks was not achieved (data not shown).

The dimer–monomer ratio in the purified insulin receptor preparation was estimated to be greater than 1 by densitometric scanning of the autoradiogram. Fractions associated with peak I ($\alpha_2\beta_2$ rich) were pooled as were fractions associated with peak II ($\alpha\beta$ rich) as shown in Figure 5. Specific activity (percent specific insulin binding per microgram of protein) of each peak was measured under our standard assay conditions (50 mM Tris-HCl, pH 7.4). The specific activity ratio of peak I/peak II was estimated to be 0.26 ± 0.02 (Table II). These results suggest that the dimer (peak I) has one-fourth of the specific activity of the monomer under the standard assay conditions (50 mM Tris-HCl, pH 7.4) used throughout this study.

Scatchard analyses of peak I and II receptors showed qualitative differences in that peak I receptors showed a curvilinear plot whereas peak II receptors a linear plot (Figure 6). The plot for peak I was best described by a two-site model in which one of the sites was involved in cooperative interactions. This model is prefered over a one-site model with cooperative interactions (P = 0.0001). The preferred fit suggests that ~86% of the total activity is attributed by the cooperative site and the remaining 14% by a noncooperative site. This is understandable since peak I receptors were possibly contaminated by peak II receptors whose Scatchard plot was best described by a one-site model without cooperative interactions. These results indicate that the binding sites in the $\alpha_2\beta_2$ form (peak I) are negatively cooperative whereas the sites in $\alpha\beta$ form (peak II) are not interacting.

Discussion

In the present study we have applied the radiation inactivation method on the purified insulin receptor to determine the functional size for insulin binding activity and to evaluate the "affinity regulator" model which has been previously proposed by one of us to explain an increase in specific insulin binding activity after expossure to low radiation doses (Harmon et al., 1980, 1981, 1983).

First, we confirmed the affinity increase phenomenon using crude Triton X-100 extracted placental insulin receptors, which is consistent with the previous observations by Harmon et al. (1980, 1981, 1983) using rat liver membranes. Second, attention was focused on the possibility that oligomeric inter-

action among receptor subunits could be affecting insulin binding activity since the purified receptor contains only α, β, and β_1 subunits as judged by SDS–PAGE under reducing conditions followed by silver staining (Fujita-Yamaguchi, 1984) and there is no evidence for a large structural protein corresponding to the putative affinity regulator.

Determination of the functional size for insulin binding activity using the purified insulin receptor turned out to be more complicated than expected, since different patterns of radiation inactivation curves were obtained depending upon the individual preparations. Despite this apparent disparity, all experimental data could be described by the same monomer–dimer model, similar to that used to describe calmodulin-dependent phosphodiesterase activity (Kincaid et al., 1981; Verkman et al., 1984). The different radiation curves observed for the purified insulin receptor can all be simulated by assuming that the receptor preparations are composed of dimers and monomers. Thus, the variability between experiments is easily explained if two variables are considered: (i) the dimer/monomer ratio and (ii) the relative insulin binding activity of dimers and monomers. In a case of calmodulin-dependent posphodiesterase, it is assumed that monomers are fully active in the absence of calmodulin whereas dimers are inactive in the absence of calmodulin. Since both $\alpha_2\beta_2$ and $\alpha\beta$ forms of the insulin receptor can be affinity-labeled with a tracer amount of ^{125}I-insulin (Fujita-Yamaguchi, 1984), both dimeric and monomeric forms of the insulin receptor are expected to have insulin binding activity. In order to compare the specific activity of the two forms, however, it is necessary to isolate each form.

Recently, Koch et al. (1986) reported the existence of two insulin receptor species with different binding properties in rat liver. Their important finding is that the insulin binding profiles of rat liver microsomal Triton extracts on Sepharose CL-6B are different depending on the assay buffer conditions: buffers of high molarity and basic pH yielded both peak I and peak II, whereas buffers of low molarity and neutral pH yielded peak II only. Buffers of intermediate molarity or pH, which are the conditions being used by most of the investigators in the field, produced one mixed peak in an intermediate position. Peak I receptors with a Stokes radius of 9.2 nm were shown to be composed of ^{125}I-insulin-labeled protein bands of M_r 400 000 by SDS–PAGE under nonreducing conditions. In contrast, peak II receptors with a Stokes radius of 8.0 nm were shown to be M_r 210 000. These values correspond well with those of $\alpha_2\beta_2$ and $\alpha\beta$ receptor forms found by others (Massague & Czech, 1982; Fujita-Yamaguchi, 1984; Velicelebi & Aiyer, 1984).

We applied affinity-purified receptors to a Sepharose CL-6B column and assayed insulin binding using our standard conditions (50 mM Tris-HCl buffer, pH 7.4, containing 0.1% Triton X-100 and 0.1% BSA) and "the buffer of high molarity and basic pH" (60 mM phosphate buffer, pH 8.0, containing 0.2 M Na_2SO_4, 0.1% Triton X-100 , and 0.1% BSA). Our results are consistent with those of Koch et al. (1986). Under standard assay conditions, competition binding assays were performed for both peak I and peak II fractions. Analysis of the binding data by the method of Scatchard revealed that peak I fractions show a curvilinear plot whereas peak II fractions yield a linear plot. Similar analyses on peak I and peak II receptors by Koch et al. (Munson & Rodbard, 1984) were not as clear in showing such a qualitative difference between the two peaks as we have observed on our receptor preparations. However, they have subsequently demonstrated that insulin-enhanced tracer dissociation was observed with peak I receptors but was not observed with peak II receptors (Deger et al., 1986). These observations are consistent with our data suggesting that a curvilinear Scatchard plot observed for peak I fractions is due to negatively cooperative interactions between insulin binding sites in the $\alpha_2\beta_2$ form as originally proposed by De Meyts et al. (1976).

Isolation of peak I and peak II receptors from our affinity-purified insulin receptors and measurement of insulin binding activity revealed that peak II receptors are more active than peak I receptors under the standard conditions. It was estimated that the specific activity (percent specific insulin binding per microgram protein) of peak I receptors is on average 26% of that of peak II receptors. However, we were not confident of the protein estimation, since we used $\sim$5–10 μg of the purified receptor for gel filtration experiments and experienced some technical difficulties in estimating protein amounts of peak I and peak II receptors in which contaminating proteins were introduced during chromatography and concentration. Alternatively, ^{125}I-labeled receptors were fractionated by Sepharose CL-6B chromatography, and each fraction was analyzed by SDS–PAGE under nonreducing conditions. The amount of the receptor was estimated by densitometric scanning of radioactive bands. According to this protein estimation, specific activity of peak I receptors is estimated to be $\sim$32% of that of peak II receptors. These studies have suggested that a monomer ($\alpha\beta$) form possesses a higher specific insulin binding than a dimer ($\alpha_2\beta_2$) form under our standard assay conditions. This is not consistent with the results recently reported by others (Boni-Schnetzler et al., 1986; Sweet et al., 1986). They showed that the monomer ($\alpha\beta$) form isolated after DTT–alkaline treatment of the receptor showed lower insulin binding activity than the intact ($\alpha_2\beta_2$) form. The $\alpha\beta$ forms we have isolated showed higher affinity (K_d = 0.26 $\pm$ 0.008 nM) than that obtained after the DTT–alkaline treatment (K_d = 1.4 $\pm$ 1 nM; Sweet et al., 1987). Therefore, we feel that the alkaline treatment they used is likely to decrease the native affinity by partial denaturation. More importantly, such a low binding affinity cannot explain our radiation inactivation results, suggesting that isolation of fully active $\alpha\beta$ forms has not been achieved by them. Our studies which are consistent with the results obtained by Koch et al. (1986) are clearly different from theirs in that we are isolating naturally occurring $\alpha\beta$ forms which are likely to exhibit full binding activity. Radiation inactivation studies described in this paper allow us to analyze activities of monomer and dimer forms in their native state without isolation of each form.

It is empirically known that the functional size calculated from radiation inactivation experiments seems to represent only the protein part of glycoprotein (Fewtrell et al., 1981; Innerarity et al., 1981; Lowe & Kempner, 1982; Haigler et al., 1985). The molecular weight of the protein portion of the α and β subunits, 152 000, has been determined from cDNA sequence data (Ullrich et al., 1985), and the molecular weights of the intact receptor ($\alpha_2\beta_2$) and half-receptor ($\alpha\beta$) have been determined as 320 000 and 195 000 by SDS–PAGE (Massague & Czech, 1982; Fujita-Yamaguchi, 1984). The functional size for the insulin binding site was M_r 227 000 $\pm$ 39 000 when target size analyses were performed on purified receptor preparations, suggesting that it represents half ($\alpha\beta$) of the intact receptor. Thus, an ionizing event occurring at either the α or β polypeptide chain apparently causes a loss in the activity of the $\alpha\beta$ monomer without significantly causing an effect on the activity of the other half of the dimer. The size estimated by the crude Triton X-100 membrane extracts was

significantly lower (M_r 102 000 ± 14 000) possibly due to the presence of proteolytically degraded binding components or of free α subunits with high affinity for insulin. It is possible that such smaller molecular weight components may be eliminated during purification by WGA- and insulin–Sepharose chromatography.

The present results suggest that the binding affinity of the insulin receptor is determined by the degree of association of receptor subunits, and they exclude the possibility previously proposed (Harmon et al., 1980, 1981, 1983) that a separate structural regulatory protein is involved. However, it should be noted that the molecular weight proposed for the affinity regulator (~300 000) may correspond to the size of the dimer which does, in fact, regulate the affinity of the binding site by its equilibrium with the monomer. Crude receptor preparations always show this affinity increase phenomenon. This phenomenon seems to be more significant in intact membranes than in the solubilized preparations (Harmon et al., 1980, 1981). Dimer/monomer (D/M) ratios in crude solubilized receptor preparations were also significantly higher than those in the purified receptor preparations, suggesting that associated forms may be the native state of the insulin receptor in plasma membranes. It has been shown that treatment of rat liver membranes with insulin, NaCl, or dithiothreitol results in the conversion of the radiation inactivation curve from a biphasic (type A) to a nonlinear (type B) or a linear (type C) inactivation curve (Harmon et al., 1981, 1983). According to our monomer–dimer model proposed in the present study, it is reasonable to assume that the role of these reagents is to dissociate the intact receptors ($\alpha_2\beta_2$) in the plasma membrane into monomers ($\alpha\beta$). In fact, it has been reported that incubation of solubilized or partially purified insulin receptors with insulin causes an increase in the lower molecular weight insulin binding component as judged by gel permeation chromatography (Maturo & Hollenberg, 1978; Ginsberg et al., 1976; Baron et al., 1981; Maturo et al., 1983). Further purification and characterization of the active $\alpha\beta$ form should facilitate understanding of structure–function relationship of the insulin receptor.

Acknowledgments

We thank Drs. C. R. Kahn, T. Maciag, J. F. Perdue, P. De Meyts, and G. A. Jamieson for valuable discussions, S. Kathuria and S. Choi for purification of the receptor, and F. Sorensen for secretarial assistance.

Registry No. Insulin, 9004-10-8.

References

Baron, M. D., & Sonksen, P. H. (1983) *Biochem. J. 212*, 79–84.

Baron, M. D., Wisher, M. H., Thamm, P. M., Saunders, D. J., Brandenburg, D., & Sonksen, P. H. (1981) *Biochemistry 20*, 4156–4161.

Boni-Schnetzler, M., Rubin, J. B., & Pilch, P. F. (1986) *J. Biol. Chem. 261*, 15281–15287.

Czech, M. P., Massague, J., & Pilch, P. F. (1981) *Trends Biochem. Sci. (Pers. Ed.) 6*, 222–225.

Deger, A., Kramer, H., Rapp, R., Koch, R., & Weber, U. (1986) *Biochem. Biophys. Res. Commun. 135*, 458–464.

De Meyts, P., Bianco, A. R., & Roth, J. (1976) *J. Biol. Chem. 251*, 1877–1888.

Ebina, Y., Ellis, L., Jarnagin, K., Edery, M., Graf, L., Clauser, E., Ou, J.-H., Masiarz, F., Kan, Y. W., Goldfine, I. D., Roth, R. A., & Rutter, W. J. (1985) *Cell (Cambridge, Mass.) 40*, 747–758.

Fewtrell, C., Kempner, E. S., Poy, G., & Metzger, H. (1981) *Biochemistry 20*, 6589–6594.

Finn, F. M., Titus, G., Horstman, D., & Hofmann, K. (1984) *Proc. Natl. Acad. Sci. U.S.A. 81*, 7328–7332.

Fujita-Yamaguchi, Y. (1984) *J. Biol. Chem. 259*, 1206–1211.

Fujita-Yamaguchi, Y., & Kathuria, S. (1985) *Proc. Natl. Acad. Sci. U.S.A. 82*, 6095–6099.

Fujita-Yamaguchi, Y., Choi, S., Sakamoto, Y., & Itakura, K. (1983) *J. Biol. Chem. 258*, 5045–5049.

Fujita-Yamaguchi, Y., LeBon, T. R., Tsubokawa, M., Henzel, W., Kathuria, S., Koyal, D., & Ramachandran, J. (1986) *J. Biol. Chem. 261*, 16727–16731.

Ginsberg, B. H., Kahn, C. R., & DeMeyts, P. (1976) *Biochem. Biophys. Res. Commun. 73*, 1068–1074.

Haigler, H. T., End, D., & Kempner, E. (1985) *J. Biol. Chem. 260*, 2178–2184.

Harmon, J. T., Kahn, C. R., Kempner, E. S., & Schlegel, W. (1980) *J. Biol. Chem. 255*, 3412–3419.

Harmon, J. T., Kempner, E. S., & Kahn, C. R. (1981) *J. Biol. Chem. 256*, 7719–7722.

Harmon, J. T., Hedo, J. A., & Kahn, C. R. (1983) *J. Biol. Chem. 258*, 6875–6881.

Harmon, J. T Nielsen, T., & Kempner, E. S. (1985) *Methods Enzymol. 117*, 65–94.

Innerarity, T. L., Kempner, E. S., Hui, D. Y., & Mahley, R. W. (1981) *Proc. Natl. Acad. Sci. U.S.A. 78*, 4378–4382.

Jacobs, S., Hazum, E., Shecter, Y., & Cuatrecasas, P. (1979) *Proc. Natl. Acad. Sci. U.S.A. 76*, 4918–4921.

Kahn, C. R., Baird, K. L., Flier, S., Grunfeld, C., Harmon, J. T., Harrison, L. C., Karlsson, F. A., Kasuga, M., King, G. L., Lang, U. C., Podskalny, J. M., & Van Obberghen, E. (1981) *Recent Prog. Horm. Res. 37*, 477–533.

Kasuga, M., Fujita-Yamaguchi, Y., Blithe, D. L., & Kahn, C. R. (1983) *Proc. Natl. Acad. Sci. U.S.A. 80*, 2137–2141.

Kincaid, R. L., Kempner, E., Manganiello, V. C., Osborne, J. C., Jr., & Vaughan, M. (1981) *J. Biol. Chem. 256*, 11351–11355.

Koch, R., Deger, A., Jack, H.-M., Klotz, K.-N., Schenzle, D., Kramer, H., Kelm, S., Muller, G., Rapp, R., & Weber, U. (1986) *Eur. J. Biochem. 154*, 281–287.

Laemmli, U. K. (1970) *Nature (London) 227*, 680–685.

LeBon, T. R., Jacobs, S., Cuatrecasas, P., Kathuria, S., & Fujita-Yamaguchi, Y. (1986) *J. Biol. Chem. 261*, 7685–7689.

Lowe, M. E., & Kempner, E. S. (1982) *J. Biol. Chem. 257*, 12478–12480.

Markwell, M. A. K. (1982) *Anal. Biochem. 125*, 427–432.

Massague, J., & Czech, M. P. (1982) *J. Biol. Chem. 257*, 6729–6738.

Massague, J., Pilch, P. F., & Czech, M. P. (1980) *Proc. Natl. Acad. Sci. U.S.A. 77*, 7137–7147.

Maturo, J. M., III, & Hollenberg, M. D. (1978) *Proc. Natl. Acad. Sci. U.S.A. 75*, 3070–3074.

Maturo, J. M., III, Hollenberg, M. D., & Aglio, L. S. (1983) *Biochemistry 22*, 2579–2586.

Munson, P. J., & Rodbard, G. (1984) in *Computers in Endocrinology* (Rodbard, G., & Forti, G., Eds.) pp 117–145, Raven Press, New York.

Pilch, P. F., & Czech, M. P. (1980) *J. Biol. Chem. 255*, 1722–1731.

Pollet, R. J., Kempner, E. S., Standaert, M. L., & Haase, B. A. (1982) *J. Biol. Chem. 257*, 894–898.

Roth, R. A., & Cassell, D. J. (1983) *Science (Washington, D.C.) 219*, 299–301.

Scatchard, G. (1949) *Ann. N.Y. Acad. Sci. 51*, 660–672.
Schlegel, W., Kempner, E. S., & Rodbell, M. (1979) *J. Biol. Chem. 254*, 5168–5176.
Sweet, L. J., Wilden, P. A., & Pessin, J. E. (1986) *Biochemistry 25*, 7068–7074.
Sweet, L. J., Morrison, B. D., & Pessin, J. E. (1987) *J. Biol. Chem. 262*, 6939–6942.
Ullrich, A., Bell, J. R., Chen, E. Y., Herrera, R., Petruzzelli, L. M., Dull, T. J., Gray, A., Coussens, L., Liao, Y.-C., Tsubokawa, M., Mason, A., Seeburg, P. H., Grunfeld, C., Rosen, O. M., & Ramachandran, J. (1985) *Nature (London) 313*, 756–761.
Velicelebi, G., & Aiyer, R. A. (1984) *Proc. Natl. Acad. Sci. U.S.A. 81*, 7693–7697.
Verkman, A. S., Skorecki, & Ausiello, D. A. (1984) *Proc. Natl. Acad. Sci. U.S.A. 81*, 150–154.
Yip, C. C., Yeung, C. W. T., & Moule, M. L. (1980) *Biochemistry 19*, 70–76.

Molecular and Catalytic Characterization of Intact Heterodimeric and Derived Monomeric Calpains Isolated under Different Conditions from Pig Polymorphonuclear Leukocytes†

Ichiro Fukui,‡ Haruhiko Toyohara,§ Kazuhiko Ito,∥ Takao Hamakubo,‡ and Takashi Murachi*,‡

Department of Clinical Science and Laboratory Medicine, Faculty of Medicine, and Department of Fisheries, Faculty of Agriculture, Kyoto University, and Blood Transfusion Service, Kyoto University Hospital, Kyoto 606, Japan

Received August 18, 1987; Revised Manuscript Received December 21, 1987

ABSTRACT: Evidence is presented of polymorphonuclear (PMN) cells derived from pig peripheral blood containing two molecular species of Ca^{2+}-dependent cysteine endopeptidases, calpains I and II, which require low and high concentrations of Ca^{2+}, respectively, for activation. Calpains I and II, purified from PMN homogenates, are heterodimers consisting of 83 plus 29 kDa and 80 plus 29 kDa subunits, respectively, which can be identified by using subunit-specific antibodies and which are identical with those of calpain species in other pig tissues and cells hitherto reported. However, a 70-kDa calpain can also be detected when pig PMN cells are disrupted by the nitrogen cavitation method under rather mild conditions, i.e., with minimal destruction of the lysosomes. Lines of evidence are presented showing that the 70-kDa species is devoid of the light subunit, that it is artificially derived from naturally occurring heterodimeric calpain I, and that the PMN cells before disruption contained no such monomeric form. The isolated 70-kDa calpain I, or monomeric artifact, requires only 1 μM Ca^{2+} for half-maximal activation, and it is less pH stable and much less heat stable than the parent heterodimeric calpain I. A possible mechanism for the production of this artifact is discussed.

Ca^{2+}-dependent cysteine endopeptidases (calpain, EC 3.4.22.17) and their specific endogenous inhibitor proteins (calpastatin) are known to be widely distributed in animal tissues (Murachi et al., 1981a; Murachi, 1983a,b). Two different types of calpain are known to exist, namely, calpains I and II, which show a low (micromolar) and high (millimolar) Ca^{2+} requirement for activation, respectively (Murachi et al., 1981b).

Calpains have been purified from various tissues of different animals [for reviews see Murachi (1983a,b)]. For some time previously, it was not clear whether calpain was a monomeric proteinase of approximately M_r 80 000 or a heterodimer of approximately M_r 110 000. The heterodimeric nature of an intact calpain molecule, either calpain I or II, was later established by chemical cross-linking experiments (Hatanaka et al., 1985), by the isolation of structurally related cDNA clones for the light (30 kDa)[1] and heavy (80 kDa) subunits (Sakihama et al., 1985; Ohno et al., 1984), and by the demonstration of the proteolytic digestibility of the light subunit during purification procedures (Mellgren et al., 1982). The extensive degradation of the light subunit during autolytic activation of a heterodimeric calpain has attracted much attention in view of the mechanism underlying the in vivo function of calpains (Inomata et al., 1985; Imajoh et al., 1986; DeMartino et al., 1986).

A monomeric calpain of 85 kDa was isolated from human PMN cells (Pontremoli et al., 1985; Pontremoli & Melloni, 1986). The authors reported that this 85-kDa monomer was the only molecular species of calpain they found in human PMN cells. This does not seem to be in accord with the general concepts hitherto accepted, i.e., that the intact form of calpain must be a heterodimer and that almost all animal tissues, with the rare exception of mammalian erythrocytes, contain two different genes for calpains I and II, respectively, both of which are also actually being expressed (Suzuki, 1987).

The present paper reports the existence of both calpains I and II of pig PMN cells in their respective heterodimeric forms

† This work was supported in part by a Grant-in-Aid for Scientific Research from the Ministry of Education, Science and Culture, Japan, and a Basic Research Grant from the Muscular Dystrophy Association, USA (to T.M.).

* Author to whom correspondence should be addressed.
‡ Department of Clinical Science and Laboratory Medicine, Faculty of Medicine, Kyoto University.
§ Department of Fisheries, Faculty of Agriculture, Kyoto University.
∥ Blood Transfusion Service, Kyoto University Hospital.

[1] Abbreviations: PMN, polymorphonuclear; DEAE, diethylaminoethyl; SDS, sodium dodecyl sulfate; psi, pounds per square inch; EGTA, ethylene glycol bis(β-aminoethyl ether)-*N,N,N',N'*-tetraacetic acid; HPLC, high-performance liquid chromatography; kDa, kilodalton; IgG, immunoglobulin G; Tris, tris(hydroxymethyl)aminomethane; EDTA, ethylenediaminetetraacetic acid.

0006-2960/88/0427-3260$01.50/0